Available online at www.sciencedirect.com
ScienceDirect
C. R. Chimie 12 (2009) 85–104
COMPTES RENDUS CHIMIE
http://france.elsevier.com/direct/CRAS2C/

Account / Revue

Nematic main-chain elastomers: Coupling and orientational behavior

Simon Krause, Frank Zander, Gerd Bergmann, Holger Brandt, Hendrik Wertmer, Heino Finkelmann*

Albert-Ludwigs-Universität Freiburg, Institut für Makromolekulare Chemie, Stefan-Meier-Straße 31, 79104 Freiburg, Germany

Received 21 May 2008; accepted after revision 21 August 2008
Available online 30 October 2008

Abstract

We summarize investigations on four different nematic main-chain elastomer systems. In the first part, the synthetic approaches towards nematic elastomers with clearing temperatures suitable for mechanical investigations are described. In the second part, the coupling between the liquid crystalline order and the chain conformation is quantified by the Landau-de Gennes coefficient U. Comparing different types of elastomers shows that the coupling depends on the type of mesogens forming the polymer backbone, and on the elastic modulus of the polymer network. In the third part, we compare the orientation behavior of the different systems under strain. ***To cite this article: S. Krause et al., C. R. Chimie 12 (2009).***

Keywords: Coupling; Elastomer; Liquid crystal; Main-chain; Nematic; Order; Orientation

1. Introduction

As early as 1975, de Gennes predicted and discussed qualitatively the extraordinary mechanical and optical properties that should be expected from nematic main-chain liquid crystalline elastomers (MCLCEs), where the mesogenic units are connected within the polymer backbone to build up the polymer network [1].

One of the most outstanding features of nematic elastomers is a reversible change in length at the nematic-to-isotropic phase transformation for monodomain samples that are macroscopically ordered with respect to the director. This change in shape is due to the coupling of the liquid crystalline order with the polymer chain conformation of the network. The coupling has been investigated in detail for LC side-chain elastomers [2,3], where the mesogenic moieties are attached as side groups to the monomer units of the network. However, only few investigations have been performed on main-chain elastomers, as suitable systems are much more difficult to realize chemically. Main-chain LC polymers typically exhibit high clearing temperatures and tend to crystallize [4]. These properties are desired e.g. to obtain highly ordered fibers with exceptional mechanical properties [5,6]. However, for detailed investigations of the mechanics of networks in the nematic state with our experimental setup, clearing temperatures not too far above ambient temperature are required. In order to perform reversible

* Corresponding author.
E-mail address: heino.finkelmann@makro.uni-freiburg.de (H. Finkelmann).

1631-0748/$ - see front matter
doi:10.1016/j.crci.2008.08.003

measurements at equilibrium conditions, no decomposition of the organic material should occur.

Several approaches are known from literature to realize crosslinked main-chain polymers. Mainly linear polymers containing a photoactive moiety have been prepared [5–10]. These functional linear polymers were crosslinked after processing. Another method described in the literature is the preparation of linear polymers bearing functional groups that are chemically crosslinked following a conventional polymerization technique [11–14]. Crosslinked materials with a high crosslinking density, the so-called thermosets, have been synthesized in a one-pot reaction. Here the repeating unit of the linear polymer and the crosslinker were reacted together in order to directly form the densely crosslinked sample [15–17]. The one-pot approach has been used as well to obtain weakly crosslinked materials by adding a flexible spacer as comonomer to the reaction mixture [18–22].

Up to now only few weakly crosslinked nematic networks are known that have been synthesized from main-chain polymers [9,13,14,19,21,23–25]. The first nematic monodomain elastomers with a permanently fixed orientation of the director were presented by Bergmann [13,26]. They enable the coupling behavior between the nematic order and the chain conformation of the network strands to be investigated. For these MCLCEs, a much stronger coupling is expected than for side-chain (SC) elastomers, where the mesogenic groups are decoupled from the network chains by flexible spacers.

Thermoelastic experiments reveal temperature dependent changes in length in the vicinity of the nematic-to-isotropic phase transformation up to 300% [14,23]. Even more pronounced effects are changes in length of up to 500%, as observed in thermoplastic elastomer fibers [27]. The coupling between the LC phase and the network can be quantified by the coupling coefficient U defined in the Landau-de Gennes theory.

If the elastomer synthesis is performed in the isotropic state – e.g. in the isotropic phase at elevated temperatures, or in the presence of an isotropic solvent –, and the sample is subsequently cooled or deswollen avoiding any external field that might cause orientation, a stable polydomain (PD) structure is observed. This nematic polydomain network exhibits macroscopically isotropic properties. It is well known from liquid crystalline SC elastomers that applying external fields on a nematic polydomain network causes a macroscopic orientation of the director that leads to a monodomain (MD) structure [28]. This orientation process results in a plateau in the stress/strain relation that reflects a very low modulus ("soft elasticity") [29]. As the monodomain is formed, the stress increases again and displays the modulus of the anisotropic network in the direction of the director. The orientation behavior of MCLCEs clearly differs from that of liquid crystalline SC elastomers with respect to the strain required to obtain a monodomain sample. Furthermore, the monodomain structure can already be obtained in the plateau region of the stress/strain curve [13,14]. Additional effects on the mechanical behavior of the elastomers, such as the removal of hairpins, have to be considered as well [30–33].

In the first part of this paper, we summarize some recent synthetic approaches to obtain nematic main-chain elastomers with nematic-to-isotropic phase transformations at temperatures suitable for long-term mechanical measurements. In the second part, the networks are analyzed with respect to deducing the coupling constant U from thermoelastic experiments and measurements of the nematic order parameter as a function of the temperature. Finally, the mechanical orientation behavior of polydomain MCLCEs is investigated.

2. Synthesis of the main-chain liquid crystalline elastomers

For MCLCEs that can be synthesized and examined easily, several aspects have to be considered. Due to the rigid rod-like mesogenic units in the polymer backbone, these systems tend to crystallize and show clearing temperatures where the polymer already starts decomposing. Furthermore, homopolymers with a regular arrangement of the monomer units along the backbone tend to exhibit smectic or other highly ordered mesophases [4]. Strategies to overcome these problems are the incorporation of kinks into the mesogens, laterally attached sidechains that act as plasticisers, or the use of flexible spacer chains between the rigid mesogenic units. These procedures are described extensively in the literature [34,35].

In 1997, Bergmann [13] applied these concepts to the synthesis of the first nematic MCLCE. He started from a semi-flexible polyether (Scheme 1), the properties of which had been reported in detail by Percec et al. in 1991 [36].

The free rotation around the central C–C bonding between the biphenyl unit and the phenyl ring gives rise to two different conformations of the mesogen. This brings about a comparatively low nematic-to-isotropic phase transformation temperature $T_{n,i}$ of around 120 °C, and

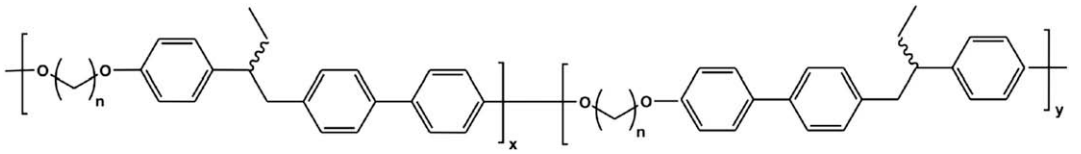

Scheme 1. Percec's [36] polyether, incorporating constitutional and conformational isomers of the repeating unit.

suppresses the formation of a smectic phase. The laterally attached ethyl spacer hinders crystallization and decreases both the clearing temperatures and the glass transition. It also creates chirality within the repeating unit and results in four different constitutional possibilities. These factors additionally decrease the crystallization tendency and enhance the solubility in standard organic solvents. With an alkyl spacer length of 10 methylene units, the system shows a broad region of the nematic phase and was chosen for the synthesis of elastomers.

Scheme 2 illustrates the synthetic approach to the elastomers. A functional linear polyether was synthesized, substituted on both ends with a rigid biphenyl moiety containing a vinyl end group. This polyether was then allowed to react with a cyclosiloxane crosslinker *via* platinum catalysis to yield the main-chain elastomers **MD-1** and **PD-1**. The monodomain elastomers **MD-1** were synthesized according to the well-known two-step reaction procedure [37], where a mechanical field is applied to the network just above the gelation point and the reaction is completed in the loaded state. The polydomains **PD-1** were synthesized without a mechanical field. It needs to be noted that the exact stoichiometry for the reaction of the polymer with the cyclic crosslinker is hard to determine. Both the measurement of the concentration of functional groups in the pre-polymer and the weighting of the volatile crosslinker bring about considerable errors. Therefore, three different polydomain elastomers **PD-1a** to **PD-1b** with slight variations of the crosslinker concentration were synthesized, the objective being to minimize the amount of material not incorporated into the network, the so-called soluble contents.

Table 1 summarizes the thermal properties and swelling behavior of the systems investigated (see chapters 3 and 4). As expected, **MD-1** displays a large swelling anisotropy Σ (with $\Sigma = (a_{perp}/a_{par}) - 1$, where a_{perp} is the degree of swelling perpendicular to the director and a_{par} is that one parallel to the director) while the polydomain samples swell isotropically. The sample **PD-1a** has a remarkably high degree of swelling q, indicating a weakly crosslinked structure. This is supported by the large soluble contents of this sample, and by the temperatures of the glass transition T_g and phase transformation $T_{n,i}$, which are close to those of the non-crosslinked polymer (where $T_g = 28\ ^\circ C$ and $T_{n,i} = 99\ ^\circ C$).

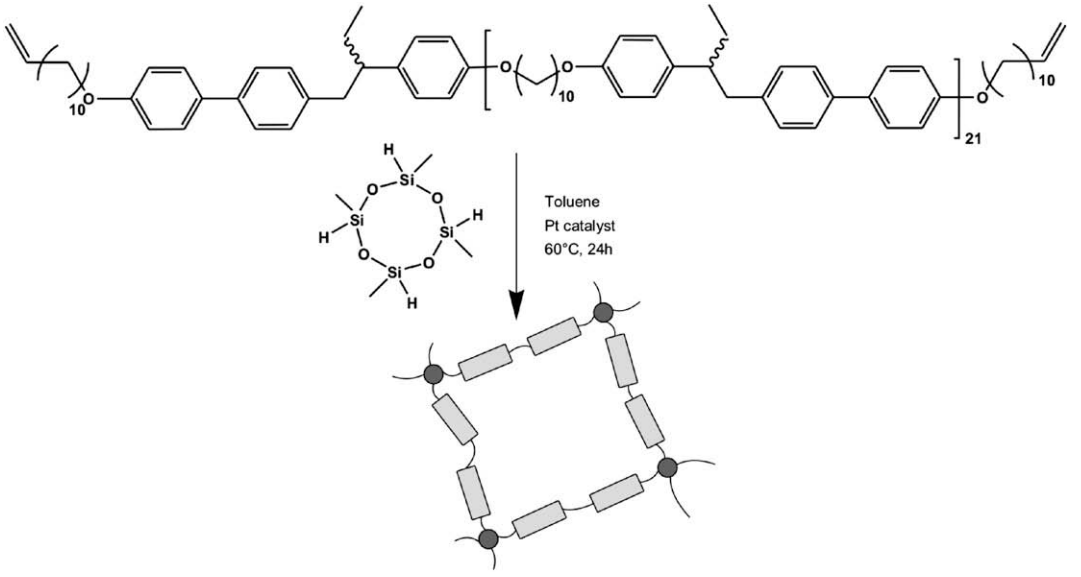

Scheme 2. Elastomer synthesis scheme of the systems **MD-1** (monodomain) and **PD-1** (polydomain).

Table 1
Thermal and swelling properties of the **MD-1** (monodomain) and **PD-1** (polydomain) systems

	T_g	$T_{n,i}$	q	Σ	Sol. cont./%
MD-1	39	122	3.2	2.8	2
PD-1a	23	96	8.4	0	61
PD-1b	36	124	1.7	0	3
PD-1c	37	114	3.2	0	3

T_g is the temperature of the glass transition, $T_{n,i}$ is the transformation temperature from the nematic to the isotropic state, q is the degree of swelling in toluene, and Σ is the swelling anisotropy ($\Sigma = (a_{perp}/a_{par}) - 1$).

In order to examine the influence of an LC elastomer's chemical constitution on its physical properties, Wermter [14] developed a co-elastomer system, where he used Bergmann's vinyl-functionalized polymer as a main-chain crosslinker for a side-chain LC polymer. Thus, he was able to control both the crosslinking density and the degree of polymerization of the crosslinker. Also, the side-chain component acts as plasticizer, further decreasing the phase transition temperature. Scheme 3 shows the general synthetic concept of these systems, where **MD-2** (monodomains) and **PD-2** (polydomains) are synthesized from the side-chain mesogen **W1**, the main-chain component **W2**, and the poly(methylhydrogensiloxane) by a platinum catalyzed addition reaction. Table 2 summarizes the composition and thermal properties of the samples, which will be discussed in chapters 3 and 4. With an increasing fraction of main-chain mesogens, both T_g and $T_{n,i}$ increase. For the monodomain samples, the swelling anisotropy Σ increases as well. The degree of swelling q is almost constant for all samples. It should be noted that the soluble contents of the elastomers were below 2%, which indicates a clean polyaddition reaction.

A different approach to obtain main-chain LCEs was proposed by Donnio et al. [19]. It is based on the chemistry of linear polymers investigated by Aguilera et al. [38]. Here, dimethyl-siloxane units are introduced to lower the phase transition temperatures. Instead of starting from pre-synthesized main-chain polymers, this synthesis is based upon a simple one-pot polyaddition reaction *via* hydrosilylation of a divinyl-substituted mesogenic monomer with tetramethyldisiloxane (TMDS) and a cyclic siloxane crosslinker (HD5). This elegant approach facilitates the access to MCLCEs, since it merely requires the preparation of a divinylic mesogenic monomer. However, the first networks prepared by this approach show smectic

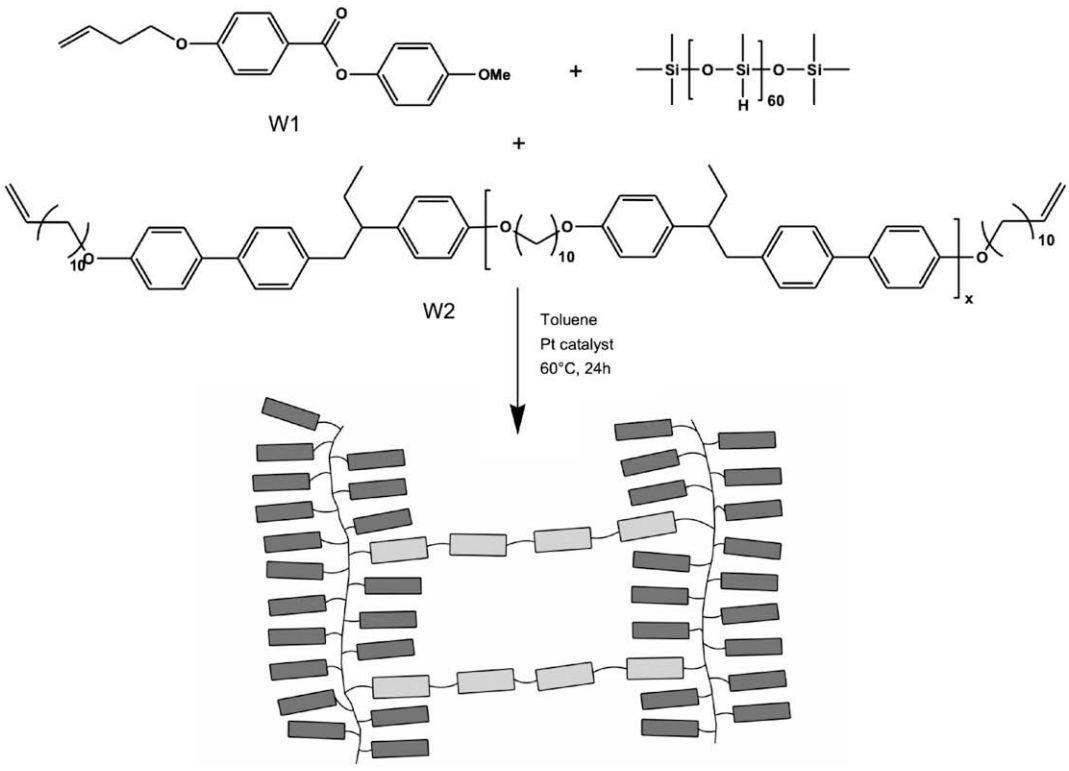

Scheme 3. Synthesis concept of the co-elastomer systems **MD-2** (monodomain) and **PD-2** (polydomain).

Table 2
Composition, thermal and swelling properties of the **MD-2** (monodomain) and **PD-2** (polydomain) systems

	Ratio of **W2** in the sample/%	Length of **W2**/ monomer units	T_g	$T_{n,i}$	q	Σ
MD-2a	20	13	7	89	6.9	1.8
MD-2b	28	13	8	86	6.3	2.9
MD-2c	46	20	13	95	6.5	4.1
MD-2d	57	26	19	96	6.8	4.5
PD-2a	20	13	3	89	6.9	0
PD-2c	46	20	11	96	6.5	0
PD-2e	77	30	24	94	6.9	0

T_g is the temperature of the glass transition, $T_{n,i}$ is the transformation temperature from the nematic to the isotropic state, q is the degree of swelling, and Σ is the swelling anisotropy.

phases at low temperatures. This is due to the symmetric structure of the mesogenic units and the tendency of the siloxane units to phase-separate.

By varying the structure of the mesogens and the length of the siloxane units, Brandt elaborated Donnio's approach (Scheme 4). Using mesogens with only two aromatic rings shift the phase transition temperature to lower values. In order to avoid the segregation of the siloxane units and the formation of a smectic phase, short vinyl chains and short-chained siloxane co-monomers were used. By co-polymerization of mesogens with different lengths of the vinyl chains, the tendency to arrange in a layered structure was additionally decreased. With these concepts, elastomers with a broad nematic phase, which exhibit practical and experimentally accessible temperatures, were realized.

Table 3 summarizes the composition, thermal and swelling properties of the systems **MD-3** (monodomain) and **PD-3** (polydomain), which will be described further in chapters 3 and 4. The sample **MD-3a** only shows a narrow nematic phase above a smectic-C phase and a smectic phase of higher order. **MD-3b** and **PD-3b**, which contain mesogens with shorter spacers, exhibit a nematic phase over a broader temperature region, but still have a smectic-C phase at low temperatures. This S_C phase is successfully suppressed in **MD-3c** by co-polymerization of mesogens with a large difference in the vinyl chain length.

Although the convenient and simple procedure of this synthesis of MCLCEs has to be emphasized, some problems need to be mentioned. An incomplete conversion of the addition reaction is caused by side reactions of the vinyl groups. These side reactions have been carefully analyzed. Furthermore, traces of monofunctional mesogens may be introduced due to impurities of the vinyl derivative used for their synthesis. The impurity and the side reactions cause a considerable amount of material that can be extracted from the network, the so-called soluble content. To overcome this problem, Krause developed a new mesogenic unit based on Donnio's three-ring central core. The laterally attached ethyl side-chain successfully suppresses a smectic phase. The vinyloxy end groups lead to a clean polyaddition reaction without side-reactions such as double-bond migration. Indeed, this concept results in elastomers with very low soluble contents. Hence, networks with low concentrations of crosslinkers, and therefore with a low elastic modulus, are synthetically accessible.

Scheme 5 shows the general synthetic concept for the **MD-4** (monodomain) and **PD-4** (polydomain) elastomers. The composition, the thermal and swelling properties, as well as the soluble contents, of the systems investigated here are summarized in Table 4. As expected, both T_g and $T_{n,i}$ increase with increasing crosslinker concentration for either monodomains or polydomains, whereas the degree of swelling q decreases. The swelling anisotropy Σ is not influenced by the crosslinker content. The soluble content varies between 2% and 14%, and is especially low for those

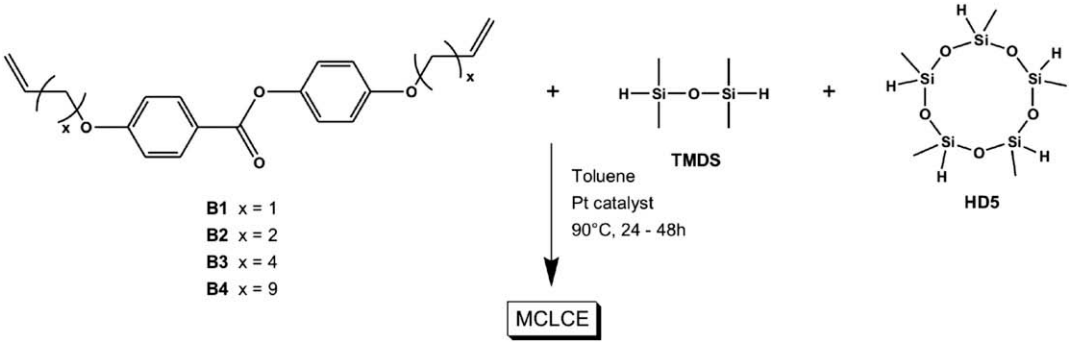

Scheme 4. Synthetic concept of the one-pot approach with two-core mesogens **B1**–**B4**.

Table 3
Composition, thermal and swelling properties of the **MD-3** (monodomain) and **PD-3** (polydomain) systems

	Mesogen	Crosslinker/%	Phase behavior	q	Σ	Sol. cont./%
MD-3a	B3	8	g 8 S_x 21 S_C 71 n 73 i	6.2	1.7	20
MD-3b	B2	10	g 3 S_C 31 n 48 i	9.2	1.7	~20
MD-3c	B1:B4 (1:1)	8	g −7 n 60 i	10.9	2.2	25
PD-3b	B2	10	g −3 S_C 28 n 43 i	6.2	0	19

q is the degree of swelling and Σ is the swelling anisotropy.

systems with a crosslinker concentration between 6% and 8%.

Over the last decade, the central synthetic goal in the field of MCLCEs has been to obtain systems with a defined and reproducible network structure, i.e. low soluble contents, with nematic phases over the whole mesophase temperature range, and with convenient phase transition temperatures. Bergmann and Wermter used pre-polymerized mesogens as main-chain parts. This approach enables the chain length of the resulting networks to be controlled precisely, but requires a two-step reaction with intermediate work-up. Brandt and Krause made use of a more flexible one-pot reaction, accepting a statistical distribution of the chain lengths and in some cases increased soluble contents.

3. Coupling

Nematic monodomain elastomers exhibit a large change in length in the vicinity of $T_{n,i}$, which is proportional to the change of the order parameter. This proportionality was experimentally verified for nematic side-chain elastomers. In order to quantify the coupling between the nematic order and the macroscopic dimensions of a nematic monodomain elastomer, the basic relations can be evaluated in the frame of the Landau-de Gennes [39,40] theory. The free energy F of a nematic network is expanded in a power series of the nematic order parameter S. The order parameter S itself is a product of S_{nematic}, describing the nematic order of the mesogens within the domains, and S_{domains}, which describes the order of the domains over the whole sample:

$$S = S_{\text{nematic}} \cdot S_{\text{domains}}$$

For monodomains, we assume $S_{\text{domains}} = 1$ and therefore $S = S_{\text{nematic}}$. According to de Gennes [1,30], the free energy expansion for crosslinked polymers takes the form:

$$F(S,T) = F_0 + \frac{a_0}{2}(T - T^*)\cdot S^2 + \frac{1}{3}B\cdot S^3 + \frac{1}{4}C\cdot S^4 \ldots - U\cdot S\cdot\varepsilon + \frac{1}{2}E\cdot\varepsilon^2 - \sigma\cdot\varepsilon \quad (1)$$

In this expression F_0 is the free energy of the isotropic phase, a_0, B, and C are constants, T is the absolute temperature, T^* is the hypothetical second-order phase transformation temperature slightly below $T_{n,i}$, E is the elastic modulus of the network at $T_{n,i}$, σ is the deformation caused by an external field, ε is the spontaneous deformation, and U is the coupling coefficient between the nematic order and the polymer network. For LC elastomers, a uniaxial mechanical field causes a deformation of the network, affecting the state of order of the mesogens, which is taken into account by the linear term in σ [28]. Even in the absence of an external mechanical

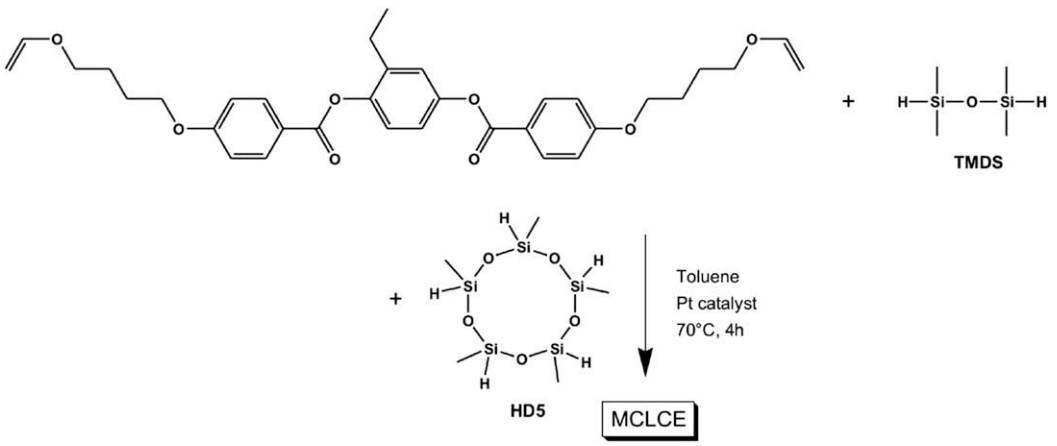

Scheme 5. Synthesis of the elastomers **MD-4** (monodomain) and **PD-4** (polydomain) with a three-ring mesogen with vinyloxy moieties in the lateral chains.

Table 4
Composition and properties of the **MD-4** (monodomain) and **PD-4** (polydomain) systems

	Content of cyclosiloxane crosslinker/%	T_g	$T_{n,i}$	q	Σ	Sol. cont./ %
MD-4a	2.5	−9	60	12.6	1.9	14
MD-4b	4.0	−8	64	8.6	2.3	10
MD-4c	6.0	−5	72	6.3	2.3	3
MD-4d	8.0	−1	84	5.4	2.1	2
MD-4e	12	6	86	4.7	2.1	9
PD-4a	2.5	−7	63	12.5	0	10
PD-4b	4.0	−5	65	7.6	0	13
PD-4c	6.0	−4	70	5.2	0	5
PD-4d	8.0	0	84	4.0	0	2
PD-4e	12	1	86	3.6	0	10

T_g is the temperature of the glass transition, $T_{n,i}$ is the transformation temperature from the nematic to the isotropic state, q is the degree of swelling, and Σ is the swelling anisotropy.

field ($\sigma = 0$), spontaneous deformations of the network occur. Minimizing expression (1) with respect to the spontaneous deformation, ε yields a spontaneous change in length under equilibrium conditions, $\varepsilon_m = US/E$ [41]. On inserting this expression into (1), the free energy expansion takes the following form:

$$F(S) = F_0 + \frac{a_0}{2}(T - T^*)\cdot S^2 + \frac{1}{3}B\cdot S^3 + \frac{1}{4}C\cdot S^4 \ldots - \frac{U^2}{2\cdot E} \qquad (2)$$

If the external field is non-zero, in addition to the spontaneous deformation another deformation of the network occurs. Minimizing (1) with respect to ε under strained conditions for small values of σ yields an equilibrium value of $\varepsilon_m = (\sigma + US)/E$.

From either equilibrium relation, one can deduce the coupling coefficient U. The plotting of the spontaneous deformation ε against the nematic order parameter S should result in a straight line. The coupling coefficient U can then be calculated from the slope of this straight line and the elastic modulus E of the isotropic network at the phase transition. Instead of the deformation ε, we use the length of the rubber referred to as the length in the isotropic state, $\lambda = L/L_{isotropic}$, where $\varepsilon = \lambda - 1$.

$$U = \frac{\partial\lambda}{\partial S}\cdot E \qquad (3)$$

This relation directly allows the determination of U by experiments and only depends on the order parameter S, the spontaneous change in length λ and the elastic modulus E of the isotropic network at the phase transformation.

In the following section we discuss how the coupling coefficient U is influenced by the chemistry of the networks described in the previous chapter. Experimentally the value of S is determined by X-ray scattering using the method described by Lovell, Mitchell and co-workers [42,43]. The elastic modulus is obtained by measuring the elastic moduli in the isotropic phase for several temperatures and extrapolating to $T_{n,i}$. Other methods have been used to calculate the coupling coefficient U, for example from the pre-transformation region above $T_{n,i}$. The authors find a difference of about one order of magnitude between the values obtained by each method [3]. In order to be able to compare the behavior of different MCLCEs, we will only use the method described above.

The first system is elastomer **MD-1** (see Table 1), a nematic main-chain polymer crosslinked *via* functional end groups. This system shows a spontaneous change in length as a function of the temperature of up to $\lambda = 3.1$ (or 210%) under load, as shown in Fig. 1(a). Extrapolating the length of the sample as a function of load, the spontaneous change in length can be evaluated for the unloaded network. The order parameter S follows the spontaneous change in length, as can be seen in Fig. 1(b) and (c). It has to be noted that – in direct analogy to side-chain elastomers – all monodomain networks exhibit a continuous change of the order parameter with temperature, which indicates supercritical behavior [28,44].

In order to calculate the coupling coefficient U, the elastic modulus of the network E is required. However, the sample **MD-1** has a clearing temperature $T_{n,i}$ of 122 °C (see Table 1). When measured under equilibrium conditions at this temperature, it decomposes with time and causes non-reproducible stress–strain curves. Hence, it was not possible to measure different moduli in the isotropic state and to extrapolate to the modulus at $T_{n,i}$. Extrapolating measurements of the moduli from lower temperatures to $T_{n,i}$ does not yield the required modulus E, either, because these moduli do not solely represent the rubber elasticity of the network. Rather, the modulus decreases with increasing temperature, reflecting the strong influence of the nematic field and not the temperature dependence of the rubber elasticity. A calculation of E *via* the ideal network theory is not reasonable due to rather large non-ideal effects of such a system even in the isotropic phase. Therefore, no reasonable quantity of U can be given for **MD-1**.

These problems clearly indicate the necessity to modify the chemistry of the systems in order to get

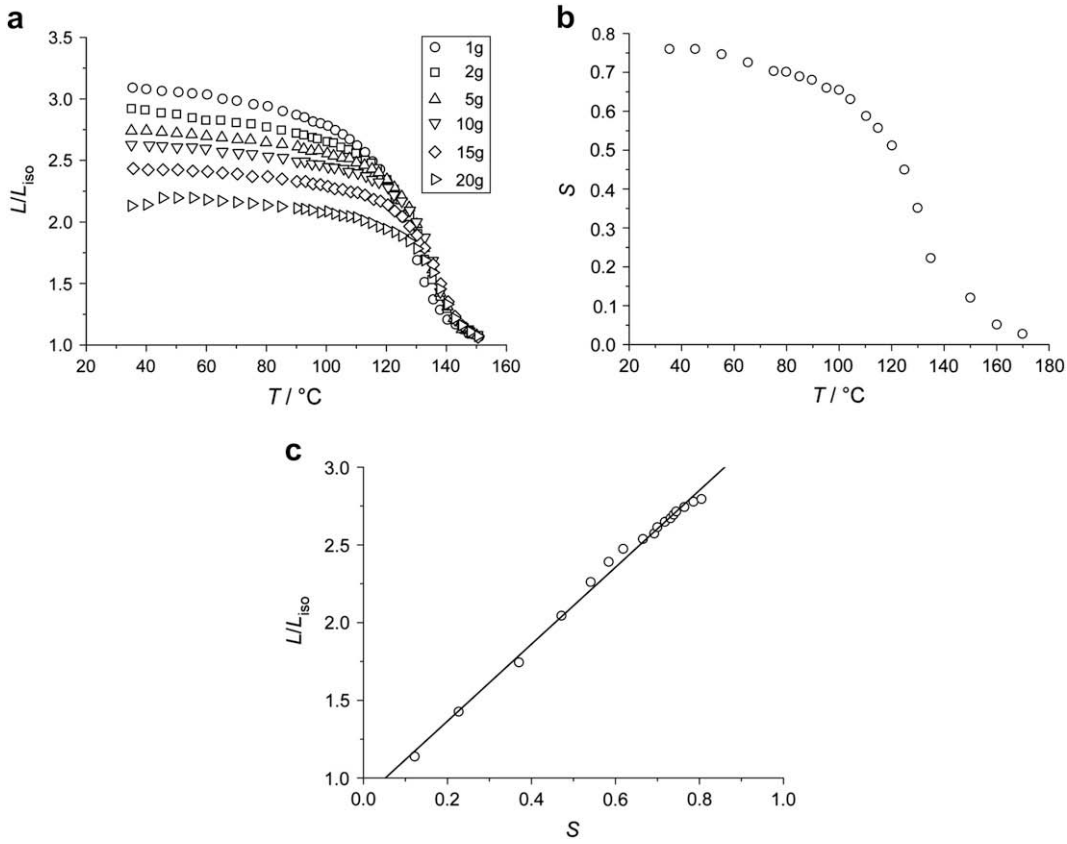

Fig. 1. (a) Spontaneous change in length λ vs. temperature measured with different loads for **MD-1**, where $\lambda = L/L_{isotropic}$. (b) Temperature dependence for the nematic order parameter S determined by X-ray for **MD-1** without load and (c) nematic order parameter S vs. change in length λ without load.

networks with a temperature regime of the nematic phase that allows obtaining reliable experimental results.

For the elastomers **MD-2a**–**MD-2d** (see Table 2), the same main-chain LC polymers are crosslinked by side-chain LC polymers. Here $T_{n,i}$ can be affected and lowered by the side-chain component. The thermoelastic experiments reveal that both a higher ratio of main-chain polymer and main-chain polymers with a higher degree of polymerization increase the spontaneous change of length to up to $\lambda = 3.8$ (or 280%) (see Fig. 2a). The effect of an increasing fraction of the main-chain polymer can be seen when elastomers **MD-2a** and **MD-2b** are compared, where the main-chain parts have the same degrees of polymerization. The effect of the chain length becomes evident when the elastomers **MD-2c** and **MD-2d** are compared. The amount of main-chain polymer is approximately constant (4 mol% vs. 4.6 mol%), but the degree of polymerization differs by 25%. Also, **MD-2c** and **MD-1** show similar changes of length, and in both cases the main-chain component has the same degree of polymerization of about 20 repeating units.

As can be seen in Fig. 2(b), the nematic order parameter is not affected by the chemical composition of the networks such as the ratio of the main-chain and side-chain parts. Therefore the slope of $\lambda(S)$ is solely determined by the spontaneous change of length. For all four elastomers **MD-2a**–**MD-2d**, a slight deviation from linearity in the plot of $\lambda(S)$ can be observed, especially at higher order parameters (Fig. 2(c)).

The elastic modulus rises with increasing amount of the main-chain component (Table 5) although the degree of swelling q remains almost constant at a value of $q \sim 6$–7 (Table 2). This is remarkable since for an increase of the fraction of the main-chain component, which has a poorer solubility, and for an increase of modulus, a decrease in q should be expected. The topology of the networks, however, is poorly understood and no simple explanation can be provided for their swelling behavior.

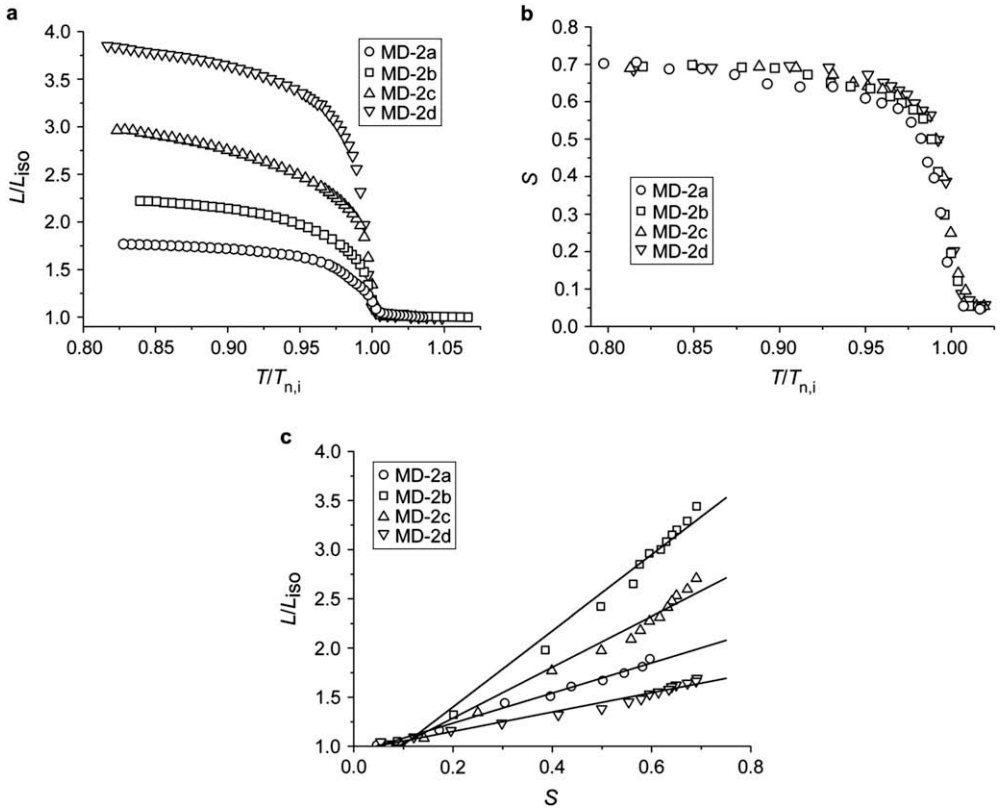

Fig. 2. (a) Spontaneous change of length $\lambda = L/L_{iso}$ plotted vs. the reduced temperature $T_{red} = T/T_{n,i}$ without load for **MD-2a**, **MD-2b**, **MD-2c** and **MD-2d**; (b) temperature dependence of the nematic order parameter S, as determined by X-ray, for **MD-2a**, **MD-2b**, **MD-2c** and **MD-2d** without load; (c) nematic order parameter S vs. change of length λ without load for these elastomers.

In the series of elastomers **MD-2**, both the slope of $\lambda(S)$ and the elastic modulus E rise upon an increasing ratio and length of the main-chain component, which result in a higher coupling coefficient. This result is reasonable and confirms the assumption that main-chain elastomers exhibit higher coupling coefficients than side-chain elastomers.

The networks **MD-3a**–**MD-3c** contain the benzoic acid phenylester, which is a short rigid mesogenic unit with two aromatic units. They are linked together *via* the tetramethyldisiloxane and alkyl chains of different length. Varying the length of these alkyl chains offers a simple approach to manipulate the phase behavior of the elastomers.

The elastomer **MD-3a**, which contains a mesogenic group substituted with a hexyl-chain, exhibits a nematic phase only in a narrow temperature region above a smectic-C phase (refer to Table 3). The thermoelastic experiments (Fig. 3a) actually reveal a shoulder in the $\lambda(T)$ curve and in a narrow temperature regime the network elongates by about 80%. The existence of the narrow nematic phase regime is also shown in detailed X-ray experiments, where the intensity of the small angle reflection as well as the correlation length of the smectic layers as a function of temperature indicate a smectic to nematic phase

Table 5
Summary of slopes of $\lambda(S)$, elastic moduli E and coupling coefficients U for all elastomers investigated

	$\frac{\partial\lambda}{\partial S}$	E [10^5 N/m^2]	U [10^5 J/m^3]
MD-1	2.6		
MD-2a	1.00	0.21	0.21
MD-2b	1.53	0.22	0.34
MD-2c	2.63	1.00	2.63
MD-2e	3.84	1.60	6.15
MD-3a	1.2 ± 0.1	3.9 ± 0.2	4.6 ± 0.5
MD-3b	1.5 ± 0.2	3.3 ± 0.2	4.9 ± 0.7
MD-3c	1.6 ± 0.2	2.1 ± 0.1	3.4 ± 0.4
MD-4a	3.0 ± 0.4	1.9 ± 0.2	6 ± 1
MD-4b	2.8 ± 0.4	2.4 ± 0.2	7 ± 1
MD-4c	2.3 ± 0.4	4.4 ± 0.4	10 ± 2
MD-4d	2.6 ± 0.3	5.9 ± 0.5	15 ± 2
MD-4e	2.4 ± 0.2	6.9 ± 0.6	17 ± 2

transformation [45]. If the thermoelastic measurements are correlated with the order parameter (Fig. 5), a linear relationship between S and λ is observed, which even covers the region of the smectic state.

The elastomer **MD-3b** differs from the previous sample by a shorter alkyl chain. Similar to the systematics of low molar mass liquid crystals, the existence of a nematic phase is favored and the temperature regime broadened compared to the previous network. Within the nematic phase the sample changes its length by about 200% (Fig. 3b), which is unaffected by the load. At the nematic to smectic phase transformation, the length of the networks remains almost constant at a decreasing temperature, which is due to the formation of the smectic layers. The change of length with temperature is now mainly determined by the thermal expansion behavior parallel to the smectic layer normal. The order parameter (Fig. 4b) follows the behavior observed for the change of length, and remains nearly unchanged within the smectic phase.

Finally, **MD-3c** only exhibits a nematic phase. The formation of the smectic order is successfully suppressed by the co-polymerization of mesogenic monomer units having different length of the flexible alkyl chains. Starting from the isotropic phase, the sample shows a pronounced change of length at the clearing temperature and continuously elongates with falling temperature (Fig. 3c). The total change of length of $\lambda = 2.2$ (or 120%) is not as large as in the case of **MD-1** or the **MD-2** systems, but clearly exceeds that of side-chain elastomers, where an elongation of $\lambda \approx 1.6$ (or around 60%) was observed. The nematic order parameter, as determined by X-ray, follows the change of length measured by thermoelastic measurements (Fig. 4c). A linear relation between the spontaneous change of length and the order parameter (Fig. 5) therefore enables the calculation of the slope of $\lambda(S)$ for all elastomers of the **MD-3** subset.

In plotting the spontaneous change of length vs. the order parameter, a linear relation is found again. A small deviation from linearity appears in the smectic phase.

For this series of elastomers the slope of $\lambda(S)$ does not seem to depend on the liquid crystalline phase, and only varies between 1.2 for **MD-3a** and 1.6 for **MD-3c**. Considering the elastic moduli (Table 5) at the nematic-to-isotropic phase transformation, the difference in the

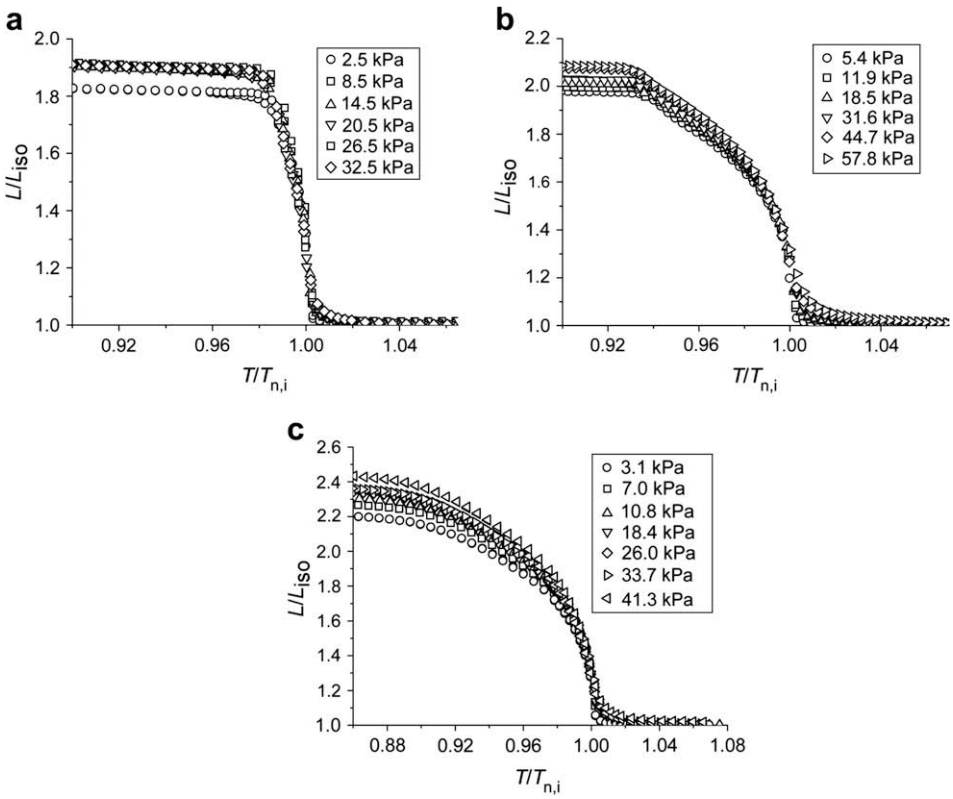

Fig. 3. Spontaneous change of length $\lambda = L/L_{iso}$ vs. the reduced temperature $T_{red} = T/T_{n,i}$ measured with different loads for (a) **MD-3a**, (b) **MD-3b** and (c) **MD-3c**. λ is referred to the length in the isotropic phase of each measurement.

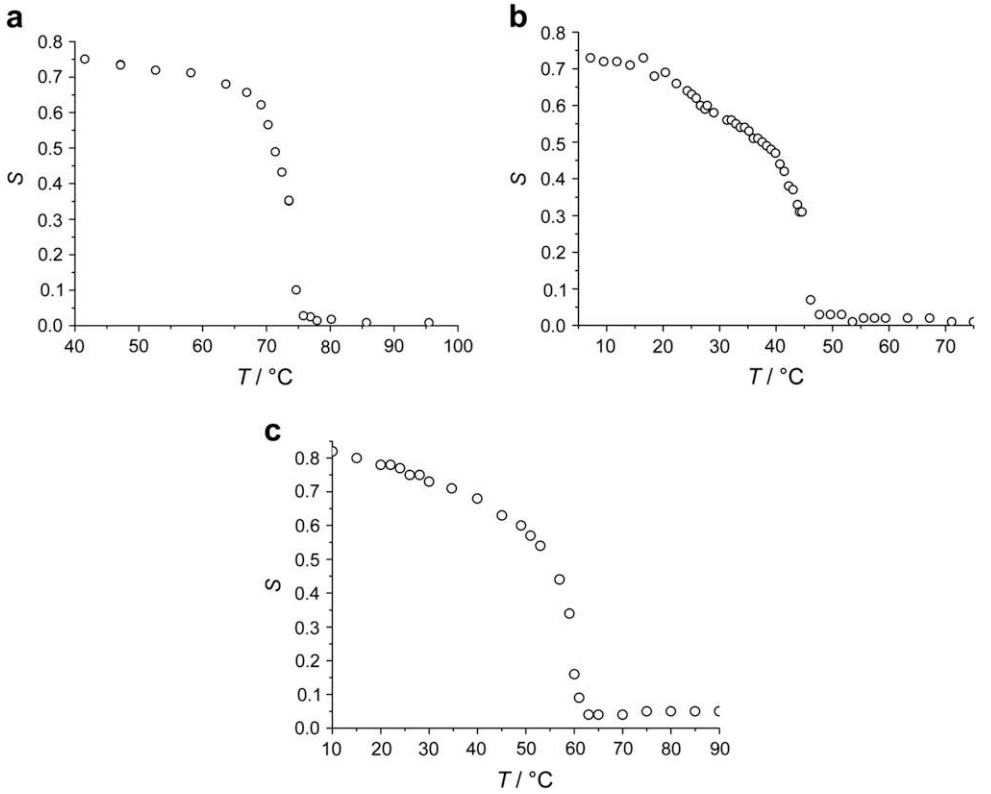

Fig. 4. Temperature dependence of the nematic order parameter S determined by X-ray without load for (a) **MD-3a** (b) **MD-3b** (c) **MD-3c**.

moduli also corresponds to the difference in the degree of swelling. A larger degree of swelling results in a lower modulus and therefore reflects lower effective crosslinking density. Obviously, for these elastomers the solubility of the networks is not affected by the change of the alkyl chain length, which is in contrast to the results obtained for the elastomers **MD-2a**–**MD-2d**. The coupling coefficients, calculated from the slope of $\lambda(S)$ and the moduli, show very similar values in the range between 3.4×10^5 J/m^3 and 4.6×10^5 J/m^3. This result is reasonable because the chemistry of the mesogenic units is not modified within this series.

In order to investigate the dependence of the coupling coefficient U on the elastic modulus, five elastomers **MD-4a**–**MD-4e** with different crosslinker concentrations were synthesized by the same one-pot reaction used for the subset **MD-3**, but with mesogenic units that contain three aromatic rings instead of two. This should lead to a stiffer polymer backbone. Additionally, by improving the polyaddition reaction by using vinyloxy-terminated monomers, we are able to vary the crosslinking density and therefore the elastic modulus of the network. This is shown by swelling experiments (Table 4), where the swelling degree increases with lower crosslinker content. The observation from the swelling behavior coincides with the mechanical investigation, where the elastic modulus in the isotropic phase increases with higher crosslinker content (Table 5). It has to be noted that the elastic moduli for the elastomers containing three aromatic unit mesogens, **MD-4a**–**e**, range from

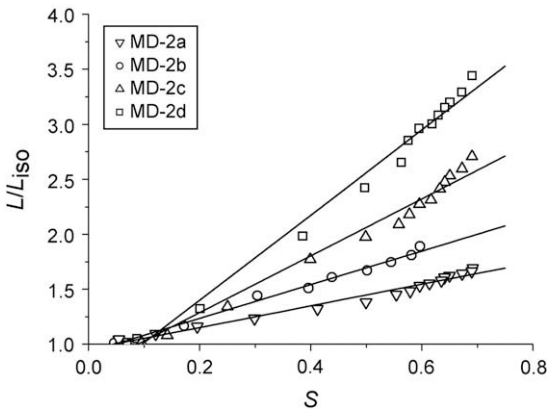

Fig. 5. Nematic order parameter S vs. change in length $\lambda = L/L_{iso}$ for the elastomer set **MD-3**.

1.9×10^5 Pa to 6.9×10^5 Pa, and are on the same order of magnitude as those for the **MD-3** series.

Fig. 6(a) shows the spontaneous change in length, measured by a thermoelastic experiment, for the elastomers **MD-4a–e** with different amounts of crosslinker. As can be seen in the curves, this series of elastomers only exhibits nematic phases. Starting from the isotropic phase, a pre-transformation regime can be seen for all elastomers. The change in length is most pronounced at the phase transformation. On further cooling, a continuous elongation is observed in the nematic phase. Comparing the change in length between the isotropic phase and a reduced temperature $T/T_{n,i} = 0.85$ for each sample, one finds a change in length of $\lambda = 2.5$ for **MD-4a** with 2.5% of crosslinker, whereas **MD-4e** with 12% of crosslinker only shows a change in length of $\lambda = 2.1$. Elastomers with longer network strands obviously exhibit larger spontaneous changes of length than highly crosslinked elastomers. The effect of the length of the network strands on the change in length is not as pronounced as in the series of the co-elastomers **MD-2a–d**.

The temperature dependence of the order parameter S for this series of elastomers is shown in Fig. 6(b). The order parameter increases within a relatively narrow temperature range when cooling from the isotropic phase into the nematic phase. Within the liquid crystalline phase, a further increase of the order parameter is observed. Similar values for the order parameter ($S = 0.70–0.76$) at $T/T_{n,i} \sim 0.85$ are found. Thus the effect of the amount of crosslinker on the order parameter is rather small. This result is surprising because the cyclic siloxane crosslinker used in these samples was expected to disturb the nematic ordering.

In order to determine the coupling coefficient, the spontaneous deformation λ is plotted against the nematic order parameter, as shown in Fig. 6(c). The plot of $\lambda(S)$ is not linear over the whole temperature range for the elastomers **MD-4a–e**. We cannot clearly judge

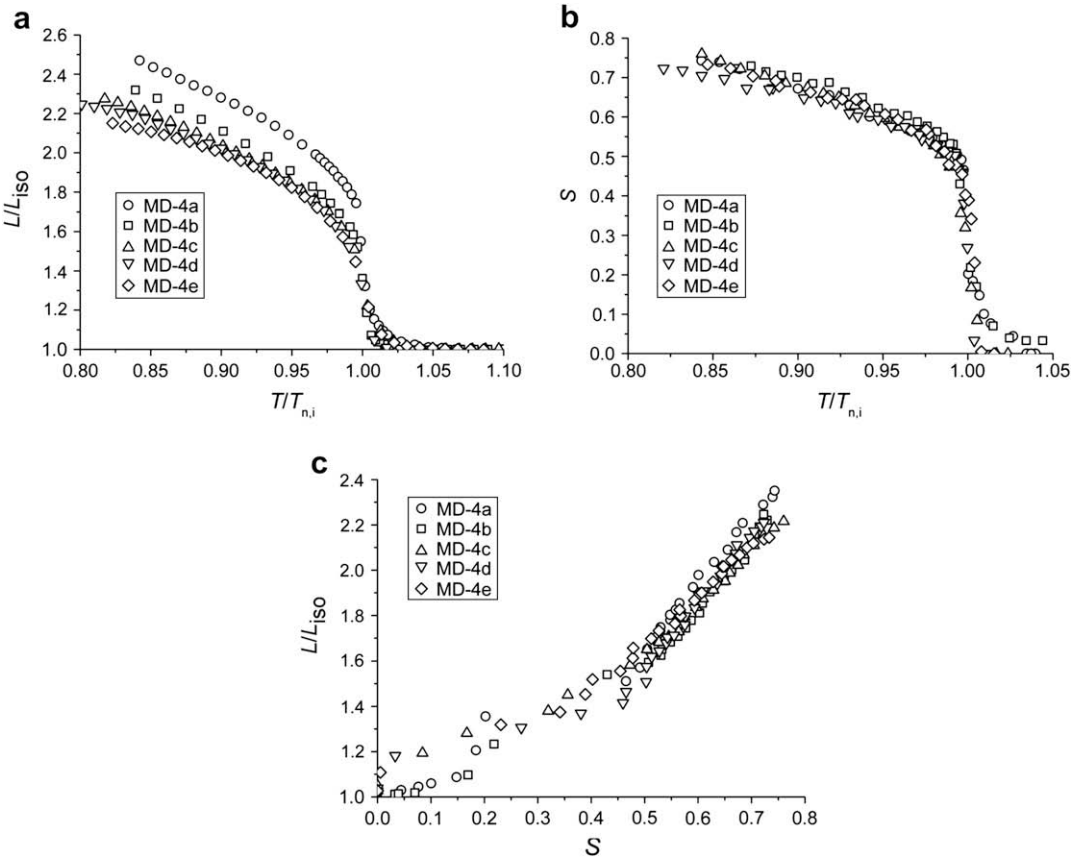

Fig. 6. (a) Spontaneous change of length $\lambda = L/L_{iso}$ vs. reduced temperature $T_{red} = T/T_{n,i}$ measured without load for all elastomers **MD-4** with different crosslinker content. λ is referred to the length in the isotropic phase; (b) nematic order parameter S determined by X-ray vs. reduced temperature $T_{red} = T/T_{n,i}$ for all samples of the subset **MD-4**; and (c) nematic order parameter S vs. change of length for all samples **MD-4**.

whether there are two linear regions or if $\lambda(S)$ is a more complicated function. The largest errors must certainly be assumed for small values of S. Additionally, the largest changes in length and in the order parameter are found in the vicinity of $T_{n,i}$, and only a small temperature mismatch between the thermoelastic and X-ray experiments will strongly affect the slope of $\lambda(S)$ in this region. We therefore determine the slope for values of $S > 0.3$. Comparing the respective values of the slopes of $\lambda(S)$ for different crosslinking densities, we find the largest value of $\partial\lambda/\partial S = 3.0 \pm 0.4$ for **MD-4a** with the lowest crosslinking density. For the elastomers **MD-4b–e**, the slope remains almost constant within the experimental error (see Table 5). The coupling coefficient U is then calculated from the elastic modulus that rises within the series **MD-4a–e**, and the slope of $\lambda(S)$, which hardly changes within this series. The coupling coefficients range from $U = 6 \pm 1 \times 10^5$ J/m^3 for **MD-4a** up to $U = 17 \pm 2 \times 10^5$ J/m^3 for **MD-4e**, as summarized in Table 5. The chemical constitution of neither the mesogenic unit nor the spacers is modified for the elastomers **MD-4a–e**. Only the amount of the crosslinker was varied. Therefore we can conclude that the coupling becomes stronger with increasing elastic modulus, as was predicted by de Gennes [30]. Comparison of the elastomers **MD-4a–e** with mesogens consisting of three aromatic units with those from **MD-3a–c** containing shorter mesogens with only two aromatic units show a weaker coupling for the two-ring systems. We speculate that the extended mesogens of **MD-4a–e** lead to a larger nematic field and a stiffening of the polymer backbone, resulting in a stronger coupling.

Neither here nor in the case of the co-elastomers of the subset **MD-2** is the relation of strain λ and order parameter S linear for higher values of S. To investigate this non-linearity in more detail, we measured the birefringence as a function of temperature for the samples with the lowest (**MD-4a**) and highest crosslinking density (**MD-4e**), respectively, using the method described by Lim and Ho [46]. A detailed description of this method, which was previously applied for the investigations on SCLC elastomers, can be found in the literature [2]. The stress applied was about 100 kPa for both samples. Fig. 7(a) shows the birefringence (on the left ordinate) and the change in length (on the right ordinate) as a function of the temperature for **MD-4a**. Starting from the isotropic phase, a distinct pre-transformation behavior is observed for the birefringence, being proportional to the nematic order parameter. Due to the high stress applied to the sample, the phase transformation is very broad. In the nematic phase, the typical continuous increase of the order parameter is observed. The change in length is defined as $\lambda = L/L_{\sigma=0,\mathrm{iso}}$, where $L_{\sigma=0,\mathrm{iso}}$ is the length of the unloaded sample in the isotropic state, and L is the length of the sample at a given temperature and stress. Comparing the change in length with the temperature dependency of the birefringence as shown in Fig. 7(a), we observe that both coincide well in the pre-transformation region and around the phase transition. However, the curve progression of the birefringence and the change in length clearly differ when going to lower temperatures. This becomes even clearer when we plot the change in length as a function of the birefringence for **MD-4a**, as shown in Fig. 7(c). At small values of birefringence, one may still observe a linear relation of $\lambda(\Delta n \sim S)$ whereas at higher values of Δn, $\lambda(\Delta n \sim S)$ deviates from linearity.

MD-4e differs from **MD-4a** in the crosslinking density. Fig. 7(b) again compares the temperature dependency of the birefringence (left ordinate) with the change in length (right ordinate) for this sample. For both measurements, a very pronounced pre-transformation region passes into the broadened phase transformation. These measurements indicate that we are here far above the critical stress. Nevertheless, both curves nicely coincide. The proportionality of the change in length and the birefringence for **MD-4e** is shown by plotting λ as a function of Δn in Fig. 7(c). The result is similar to the observations made in SCLCEs. Obviously it depends on the crosslinking density or on the length of the network strands in LCMCEs whether the coupling is linear or not. We assume that in elastomers with long network strands, and especially at higher temperatures, the network will tend to recover some entropy by forming hairpin defects. This backfolding of the polymer backbone was first predicted by de Gennes [30], and theoretically described by Warner et al. [31,32,47,48]. The first experimental evidence of this particular chain conformation in linear polymers was obtained by neutron scattering experiments [33]. By cooling an elastomer with low crosslinking density below the phase transformation temperature, some chains may form hairpins. By further cooling, these hairpins are removed due to the external field leading to an additional extension of the sample. This could explain the non-linearity in coupling behavior observed for **MD-4a**, while in the sample **MD-4e** with a high crosslinker content the network strands are too short to form hairpins, and therefore a linear coupling is observed.

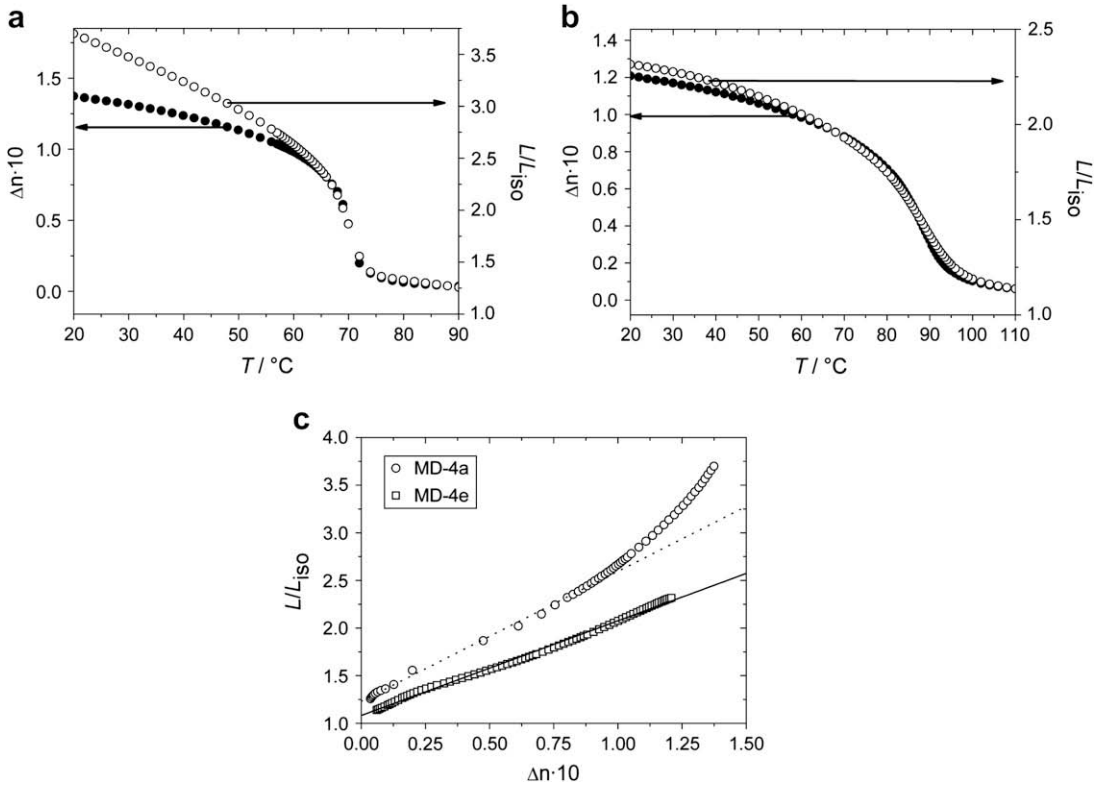

Fig. 7. Birefringence Δn (left ordinate) and change in length $\lambda = L/L_{iso}$ (right ordinate), referred to the length of the unloaded sample in the isotropic phase for (a) **MD-4a** and (b) **MD-4e**. The measurements were carried out with an external stress of ~100 kPa. (c) Spontaneous change in length $\lambda = L/L_{iso}$ from thermoelastic experiments vs. the birefringence Δn from temperature dependent measurements for **MD-4a** with the lowest and for **MD-4e** with the highest crosslinker content.

3.1. Discussion of the coupling behavior

The elastomer prepared from an end-functionalized linear polymer, **MD-1**, shows a remarkable change in length of $\lambda = 3.1$ (210%). A similar change in length is observed for the combined MC/SC elastomer **MD-2c** prepared from MC polymers with a similar degree of polymerization. Within the series **MD-2**, one can clearly see that with increasing either the molecular weight or the concentration of the main-chain component, larger changes in length are achievable (up to $\lambda = 3.8$, or 280%). This effect of longer network strands on the change in length is also observed in the elastomers **MD-4a–e**, prepared *via* a one-pot reaction, but here it is less pronounced. An explanation may be the polydispersity of the network strands in the latter system. If most of the strain is taken up by deforming short chains, the deformation of longer chains becomes less important. Another aspect is the role of the crosslinker in the mixed system **MD-2a–d**. The large deformations observed in these systems could be explained by considering the side-chain component to be a highly anisotropic, multifunctional crosslinker that contributes to the anisotropy of the network chains of the whole sample. Such a contribution is not possible for the isotropic crosslinker used for **MD-4a–e**. For the elastomers **MD-3a–c**, elastomers with different liquid crystalline phases were investigated. The changes in length of these elastomers are almost independent of the phase behavior.

For all elastomers, similarly high values of the order parameter S between $S = 0.7$ and $S = 0.8$ were observed at lower temperatures. In the combined MC/SC elastomers, the order parameter is almost independent of the amount of main-chain component. Also the concentration of the cyclic crosslinker does not affect the state of order, as seen in the series **MD-4a–e**. This is surprising because an isotropic impurity should be expected to lower the nematic ordering. In addition, the liquid crystalline phase that the elastomer exhibits – whether smectic or nematic – has little impact on the order parameter, as shown for the elastomers **MD-3a–c**.

Considering the independence of the order parameter of these factors, the slope $\partial\lambda/\partial S$ is mostly determined by

the elastomer's change in length. We observe the same slope $\partial\lambda/\partial S$ when we compare the end-linked elastomer **MD-1** and the combined elastomer **MD-2c**, but this might be coincidental. The more main-chain mesogens the elastomers of the series **MD-2a–d** contain, the larger the slope $\partial\lambda/\partial S$ is. But already in this series a deviation from linearity of $\lambda(S)$ is observed. A more detailed investigation by means of birefringence for two elastomers with different crosslinker content, **MD-4a** and **MD-4e**, was therefore performed. It shows that $\lambda(S)$ clearly deviates from linearity for an MC elastomer with long network strands, whereas a linear relation is observed for the elastomer with short network strands. We assume that the deformation of hairpins has to be taken into account here. For a main-chain system that additionally shows smectic phases, **MD-3a–c**, the linear relation of $\lambda(S)$ holds even in the smectic phase.

Comparing the coupling coefficients for the combined elastomers **MD-2a–d**, we find a stronger coupling with increasing contents of main-chain mesogens. The coupling coefficients range from 2.1×10^4 J/m^3, a value typical for side-chain elastomers, to 6.15×10^5 J/m^3. The largest coupling coefficients, however, are observed in the elastomers synthesized *via* a one-pot reaction, where values as high as $U = 1.7 \times 10^6$ J/m^3 were found. We therefore conclude that main-chain elastomers generally show a stronger coupling than side-chain elastomers. The coupling is not affected by possible smectic phases at lower temperatures (series **MD-3a–c**).

If we compare elastomers synthesized *via* a one-pot reaction, the chemical structure of the mesogens plays an important role. Elastomers with mesogens that consist of three aromatic units (series **MD-4a–e**) show a stronger coupling than elastomers with mesogens of two aromatic units (series **MD-3a–c**), independent of the crosslinker content. We explain this observation with a larger nematic field for more extended mesogens that leads to a stiffer polymer backbone and a stronger coupling. By varying the crosslinker content, and thereby the elastic modulus in series **MD-4a–e**, we find that the coupling is mostly determined by the elastic modulus of the network as predicted by de Gennes.

4. Orientation behavior

In contrast to the transparent monodomain samples, polydomains are optically opaque, indicating a microscopic structure on a length scale of the wavelength of visible light. The term *polydomain* itself may be misleading because typically, no sharp domain boundaries are observed, but rather a continuous change of the orientation of the local director. From side-chain LCEs it is well known that by applying a mechanical field, a macroscopic orientation of the local directors occurs. In mechanical experiments on these systems, this orientation process causes a soft plateau with a very low modulus up to an elongation λ_2, where the modulus rises again. Measurements of the order parameter for polydomain SCLCEs show that λ_2 is equal to the elongation λ_M where the sample achieves the structure of a monodomain [28]. Also, in the case of SCLCEs, the width of the plateau decreases with increasing temperature [28,49]. In this chapter, we explore the orientation behavior of MCLCEs.

In Fig. 8(a) the stress is plotted against the imposed strain for the polydomain elastomer **PD-1a**, prepared from end-functionalized main-chain polymers by Bergmann et al. For deformations up to $\lambda_2 \sim 5$ (or 400%), a soft response with a low modulus is observed. This exceeds by far the width of the soft plateau observed in side-chain elastomers, which show values of about $\lambda_2 \sim 1.6$ [50]. In Fig. 8(b), the plot of the order parameter S, as determined by X-ray measurements, vs. the imposed strain λ shows a saturation of S, i.e. a monodomain structure, already at a deformation of $\lambda_M \sim 2.5$. Thus, in this main-chain system, λ_2 considerably deviates from λ_M, quite in contrast to the observations made in side-chain elastomers. An explanation for this remarkable behavior may be that the additional deformation with a low modulus originates in the presence of hairpin defects. Hairpins can be straightened into fully stretched chains by an external strain with a low modulus and without significant increase of the order parameter.

The temperature dependence of the stress–strain measurements differs from that observed in side-chain elastomers as well. Fig. 8(c) shows for the case of **PD-1c** that with increasing temperature, the plateau of soft deformation broadens. As the anisotropy of the network coils is a function of temperature *via* the order parameter, one should expect a decrease of the plateau width at rising temperatures. If hairpins are present, however, they may partially retain the entropy of the polymer backbone, and a larger number of hairpins and a longer plateau should be expected at higher temperatures. Considering the temperature dependence of the plateau width, one may therefore conclude that for the elastomer **PD-1c**, the effect of the hairpins dominates the effect of the order parameter.

The co-elastomers **PD-2** synthesized by Wermter et al. (see Scheme 3 and Table 2) also exhibit a broad soft plateau up to a deformation of about 300%. Fig. 9(a) shows the plots of the nominal stress against the imposed strain for three polydomain samples. In

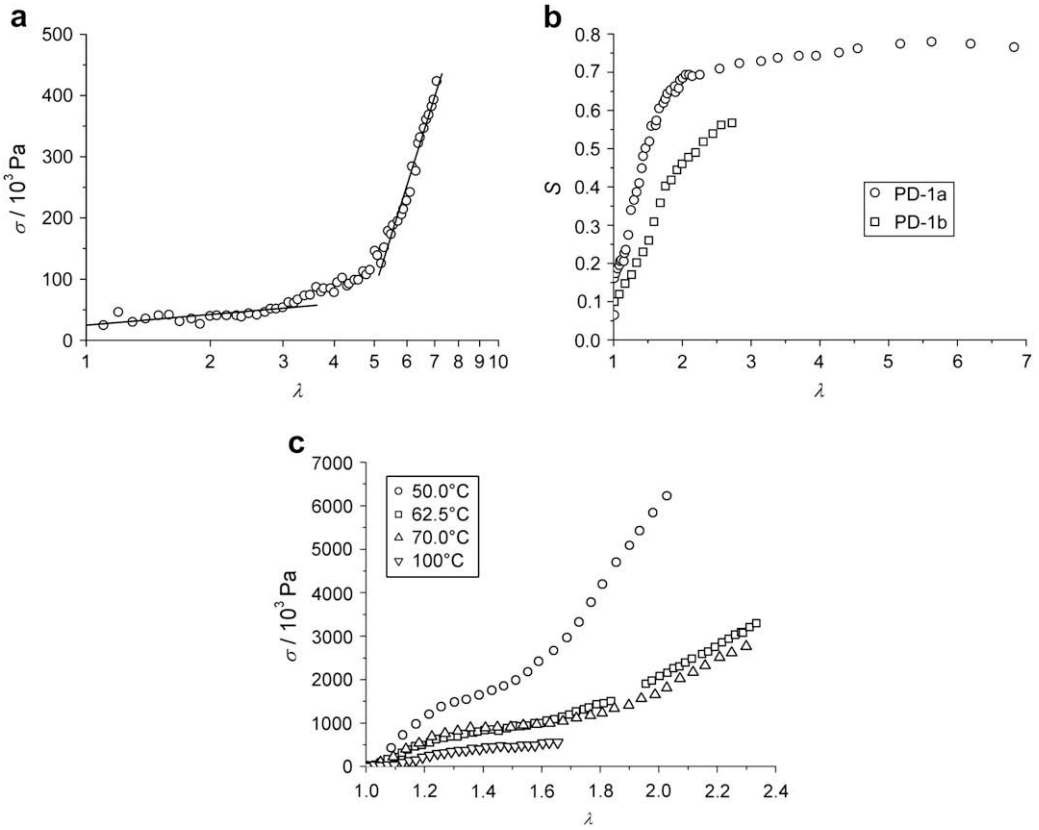

Fig. 8. (a) Nominal stress σ vs. imposed strain $\lambda = L/L_0$ for **PD-1a** at 70 °C in the nematic phase; (b) nematic order parameter S determined by wide angle X-ray scattering vs. imposed strain λ for **PD-1a** and **PD-1b**; (c) nominal stress σ vs. imposed strain λ for **PD-1c** at 50 °C, 62.5 °C, 75 °C and 100 °C.

these elastomers, two effects affect the width of the plateau: the content of main-chain polymer and its molecular weight. The increase of either of these leads to broader plateaus. We find values of $\lambda_2 = 2.3$ for the sample **PD-2a**, $\lambda_2 = 2.7$ for **PD-2c**, and $\lambda_2 = 4.0$ for **PD-2e**. In Fig. 9(b), the order parameter S under deformation, as determined by X-ray investigations, is shown. The elongations necessary for a monodomain, λ_M, are 1.7, 1.8, and 1.9 for the samples **PD-2a**, **PD-2c**, and **PD-2e**, respectively. They are determined as the intersection points of the fits to the two linear regions of the curves. Obviously, λ_M is almost independent of the composition of the system. Just like in the system **PD-1a** discussed above, there is large discrepancy between λ_2 and λ_M for these co-elastomer systems.

As for **PD-1c**, the temperature dependence of the plateau width was investigated for the sample **PD-2a** by X-ray and stress–strain measurements. Fig. 10(a) shows the stress–strain plots for different reduced temperatures $T_{red} = T/T_{n,i}$ between 0.892 and 1.00 (the phase transformation temperature). At a low temperature of $T_{red} = 0.892$ (which is still 40 °C above the glass transition), no plateau was found in the mechanical investigation. Probably the mechanical relaxation of the sample becomes so slow that the measurements were not carried out under complete equilibrium conditions. Upon increasing the temperature to $T_{red} = 0.92$, a slight non-linearity in the stress–strain curves indicates the occurrence of a plateau. Measurements at higher temperatures then clearly show a mechanical plateau that broadens with increasing temperature from $\lambda_2 = 2.0$ at $T_{red} = 0.947$ up to $\lambda_2 = 2.4$ at $T_{red} = 0.975$. The progression of the order parameter under deformation is shown in Fig. 10(b). Again, λ_M is determined as the intersection points of the fits to the two linear regions of the curves. S is independent of temperature and a saturation is always observed at $\lambda_M = 1.7$. One may speculate that the increase of the values of λ_2 with increasing

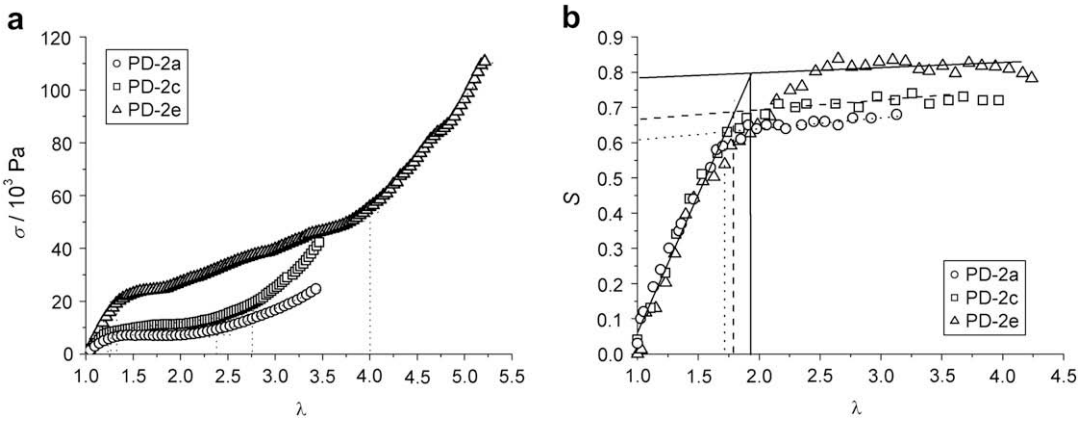

Fig. 9. (a) Nominal stress σ_n vs. imposed strain $\lambda = L/L_0$ dependent on the quantity of main-chain component in co-elastomers **PD-2a**, **PD-2c** and **PD-2e** at $T_{red} = T/T_{n,i} = 0.950$. (b) Nematic order parameter S determined by wide angle X-ray scattering vs. imposed strain λ for **PD-2a**, **PD-2c** and **PD-2e**.

temperature is again associated with hairpin defects in the main-chain component of the network, which are more likely to occur at higher temperatures.

Fig. 11(a) shows the results of stress–strain measurements at different temperatures of the elastomer **PD-3b** synthesized in a one-step reaction by Brandt et al. The order parameter S as a function of imposed strain is shown in Fig. 11(b), with λ_M again determined as the intersection of fitting lines to the linear regions of the curves. For this sample, the plateau width is much smaller than for the elastomers prepared from the end-functionalized polymers by Wermter (**PD-2**) or Bergmann (**PD-1**), but λ_2 is still larger than λ_M. At 35 °C, S saturates at $\lambda_M = 1.4$ and the modulus starts rising again at $\lambda_2 = 1.7$, and at 40 °C we observe $\lambda_M = 1.3$ and $\lambda_2 = 1.5$. The deformation λ_M here decreases with higher temperature. Remarkably, the end of the plateau λ_2 decreases with rising temperature as well, in contrast to the observations from the **PD-1** and **PD-2** systems. As the plateau width is determined, in part, by the anisotropy of the network strands, which is in turn associated with the order parameter, the effect of the network anisotropy on the mechanical properties seems to be larger for this elastomer than the effect of hairpins. In fact, the probability of hairpin backfolding depends strongly on the length of the network strands. As **PD-3b** has a higher elastic modulus and was synthesized with a large amount of crosslinker, short strands and few hairpins should occur, and a behavior like the one observed is indeed expected.

The elastomers of the series **PD-4** were prepared *via* the same one-pot synthesis as those of the **PD-3** subgroup. The main difference is a significantly lower amount of crosslinker for the case of **PD-4a** than for all samples of **PD-3**. Fig. 12(a) shows the stress–strain behavior for **PD-4a** as a function of temperature. The plateau length decreases with higher temperatures

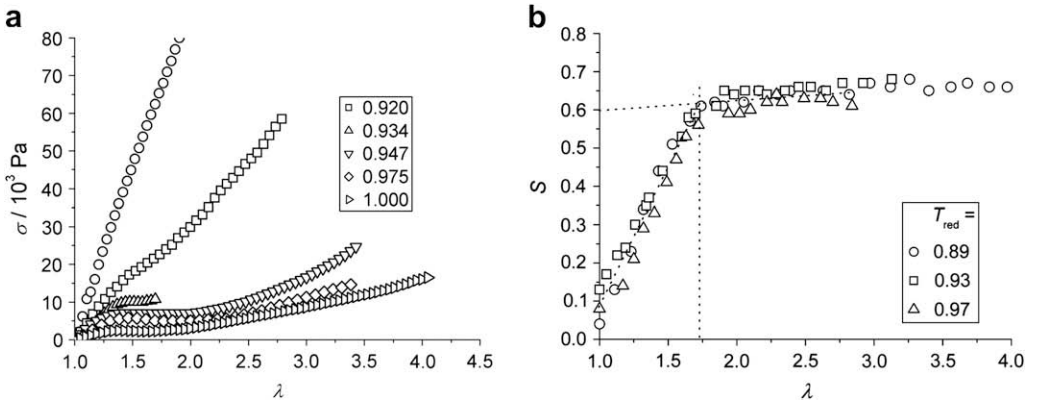

Fig. 10. (a) Nominal stress σ vs. imposed strain $\lambda = L/L_0$ at different temperatures of **PD-2a**. (b) Nematic order parameter S determined by wide angle X-ray scattering vs. imposed strain λ for **PD-2a** at different temperatures.

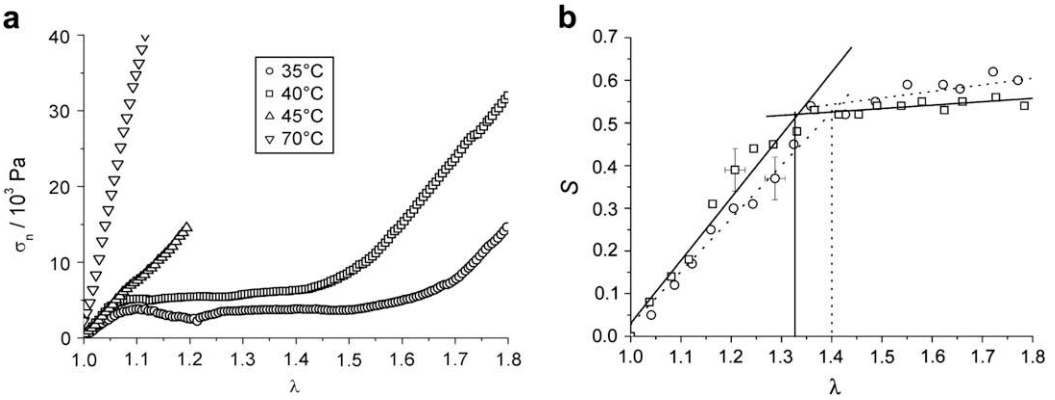

Fig. 11. (a) Nominal stress σ_n vs. imposed strain $\lambda = L/L_0$ of **PD-3b** at different temperatures indicated in the figure; (b) nematic order parameter S determined by wide angle X-ray scattering vs. imposed strain λ for **PD-3b** at 35 °C and 40 °C.

(from $\lambda_2 = 2.05$ at 30 °C to $\lambda_2 = 1.6$ at 60 °C), following the tendency observed for **PD-3b**. Assuming long network strands due to a low crosslinker concentration, and therefore the presence of hairpins, we would expect the opposite temperature dependence. Obviously, the question how the network is formed – either by using polymers that are subsequently crosslinked, or by reacting all components in one step – is very important for the system's orientation behavior.

In Fig. 12(b), the mechanical stress and the progression of the order parameter S are plotted against the imposed strain λ for a temperature of 30 °C. Already at a deformation of only about 10%, the order parameter reaches a value of about 0.3. In the plateau region of the stress–strain curve, a slight increase of the order is found. The full orientation, where the order parameter remains constant within the experimental error, corresponds to the end of the plateau. In contrast to all types of main-chain elastomers discussed above, we here find $\lambda_2 = \lambda_M$. If hairpins are at all present in these elastomers, the two processes of director orientation and hairpin removal cannot be separated, but rather happen simultaneously.

The influence of the crosslinker content on the orientation behavior is shown in Fig. 13. The width of the plateau decreases with increasing crosslinker content from $\lambda_2 = 2.04$ for **PD-4a** with the lowest crosslinking density to $\lambda_2 = 1.79$ for **PD-4e** with the highest amount of crosslinker. Thus the amount of crosslinker only seems to have a small impact on the width of the plateau, and therefore on the orientation behavior of the systems.

4.1. Discussion of the orientation behavior

For all investigated MCLCEs, we found much higher values for the end of the soft plateau, λ_2, than for side-chain elastomers. The networks synthesized from linear polymers, crosslinked either by a multifunctional crosslinker or by side-chain polymers, show similar orientation

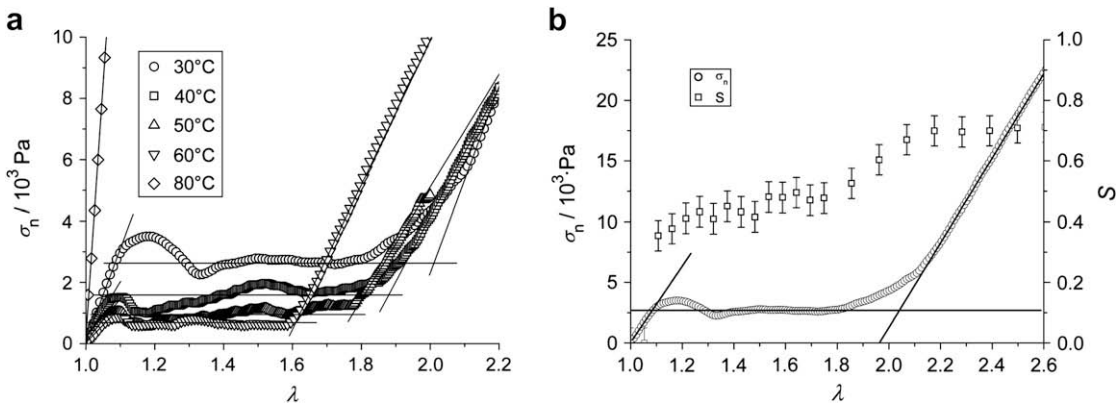

Fig. 12. (a) Nominal stress σ_n vs. imposed strain $\lambda = L/L_0$ of **PD-4a** at different temperatures indicated in figure. (b) Nominal stress σ_n (ordinate to the left) and nematic order parameter S determined by wide angle X-ray scattering (ordinate to the right) vs. imposed strain λ for **PD-4a** at 30 °C.

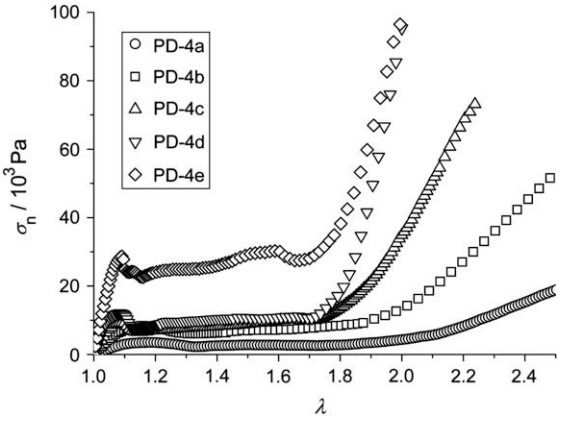

Fig. 13. Nominal stress σ_n vs. imposed strain $\lambda = L/L_0$ of the series with different crosslinker content **PD-4a**, **PD-4b**, **PD-4c**, **PD-4d**, and **PD-4e** at the reduced temperature $T/T_{n,i} = 0.91$.

behaviors: the orientation of the local directors to a monodomain at the elongation λ_M is already achieved clearly before the stress rises again at λ_2. This soft plateau is narrower for elastomers synthesized *via* a one-pot reaction. Furthermore, the two one-pot systems we investigated differ. A difference between λ_M and λ_2 was seen for the **PD-3b** elastomer, but for the elastomers with a low crosslinker content from the **PD-4** subset, the full orientation and the end of the soft plateau coincide. If the finding that λ_M is unequal to λ_2 is indeed related to hairpins, two different processes might occur. In the first one, the orientation of the domains happens first, and subsequently the hairpins are removed without further increase of the order parameter. In the second one, both mechanisms take place simultaneously. Thus, the orientation behavior cannot merely be related to the network topology, but other aspects such as the crosslinking process or the curing temperature have to be considered as well.

The temperature dependence of λ_2 obtained from stress–strain experiments shows a more general trend. Elastomers synthesized *via* the one-pot strategy exhibit shorter plateaus than elastomers synthesized *via* linear polymers that are subsequently crosslinked. In the first case, where we assume a broad distribution of the length of the network strands, the anisotropy of the network governs the length of the plateau. For the latter case, likely with a more homogeneous distribution of the network strands, hairpins seem to play a more important role.

5. Conclusion

We reported on the synthesis, coupling and orientation behavior of four series of MCLCEs developed in our group. Crosslinking end-functionalized main-chain polymers yielded the first fully nematic main-chain elastomers with moderate clearing temperatures. Co-elastomer systems where the main-chain part acts as a crosslinker of variable length and concentration showed extraordinarily high changes in length at phase transformation of up to 280%. A one-pot hydrosilylation reaction was developed as a more elegant approach to MCLCEs. Very thorough reactions and large changes in length could be achieved *via* this route when vinyl ethers were used as polymerizable moieties. By this means, it became possible to vary the crosslinking density in a very defined manner.

The coupling of the nematic order and the rubber network was quantified by the coupling constant U. The order parameter S as a function of temperature showed almost the same behavior for all systems investigated, so the slope of $\lambda(S)$ was mainly determined by the change in length λ of the samples. We showed that non-linearity in the progression of $\lambda(S)$ is observed for systems with long network strands and may be related to hairpin defects. For the co-elastomer systems, the slope of $\lambda(S)$ becomes steeper with increasing content of main-chain mesogens, as does the elastic modulus E. For the one-pot systems, an increasing value of E coincides with a decrease in the slope of $\lambda(S)$. In this case, however, E compensates for $\lambda(S)$, and thus the coupling constant U shows the same progression as E for all systems investigated. We were also able to show that $\lambda(S)$ is independent of the particular liquid crystalline phases the elastomer exhibits, and remains linear within a smectic phase. We observed higher coupling constants in one-pot systems with three aromatic rings in the mesogens than in those with only two, reflecting the higher stiffness of these mesogens and the larger the nematic field they cause.

In orientation experiments on polydomain samples, we found much broader plateaus in the stress–strain curves than for side-chain systems. For the subsets synthesized from functionalized polymers, we observe a large difference between the point where the modulus rises again, and the point where a monodomain is achieved. We ascribe this behavior again to the presence of hairpin defects. This difference is considerably smaller for the one-pot system with two aromatic cores, and completely vanishes for the vinyloxy system, probably because the orientation and removal of hairpins happen at the same time and not successively.

References

[1] P.G. de Gennes, C. R. Acad. Sci. B: Phys. 281 (5–8) (1975) 101.

[2] A. Greve, H. Finkelmann, Macromol. Chem. Phys. 202 (14) (2001) 2926.
[3] W. Kaufhold, H. Finkelmann, H.R. Brand, Makromol. Chem. 192 (11) (1991) 2555.
[4] C.K. Ober, J.-I. Jin, W.R. Lenz, Adv. Polym. Sci. 59 (1983) 103.
[5] C.H. Lin, M. Maeda, A. Blumstein, J. Appl. Polym. Sci. 41 (5–6) (1990) 1009.
[6] J. Jegal, A. Blumstein, J. Appl. Polym. Sci. 68 (3) (1998) 387.
[7] D. Creed, A.C. Griffin, J.R.D. Gross, C.E. Hoyle, K. Venkataram, Mol. Cryst. Liq. Cryst. 155 (1988) 57.
[8] P. Beyer, E.M. Terentjev, R. Zentel, Macromol. Rapid Commun. 28 (14) (2007) 1485.
[9] S. Krause, R. Dersch, J.H. Wendorff, H. Finkelmann, Macromol. Rapid Commun. 28 (21) (2007) 2062.
[10] R. Ishige, M. Tokita, Y. Naito, C.Y. Zhang, J. Watanabe, Macromolecules 41 (7) (2008) 2671.
[11] R. Zentel, G. Reckert, Makromol. Chem. 187 (8) (1986) 1915.
[12] K.H. Hanus, W. Pechhold, F. Soergel, B. Stoll, R. Zentel, Colloid Polym. Sci. 268 (3) (1990) 222.
[13] G.H.F. Bergmann, H. Finkelmann, V. Percec, M.Y. Zhao, Macromol. Rapid Commun. 18 (5) (1997) 353.
[14] H. Wermter, H. Finkelmann, e-Polymers 13 (2001).
[15] G.G. Barclay, S.G. Mcnamee, C.K. Ober, K.I. Papathomas, D.W. Wang, J. Polym. Sci.: Polym. Chem. 30 (9) (1992) 1845.
[16] G.G. Barclay, C.K. Ober, K.I. Papathomas, D.W. Wang, J. Polym. Sci.: Polym. Chem. 30 (9) (1992) 1831.
[17] M. Giamberini, E. Amendola, C. Carfagna, Mol. Cryst. Liq. Cryst. A 266 (1995) 9.
[18] C. Ortiz, M. Wagner, N. Bhargava, C.K. Ober, E.J. Kramer, Macromolecules 31 (24) (1998) 8531.
[19] B. Donnio, H. Wermter, H. Finkelmann, Macromolecules 33 (21) (2000) 7724.
[20] I.A. Rousseau, P.T. Mather, J. Am. Chem. Soc. 125 (50) (2003) 15300.
[21] D. Ribera, M. Giamberini, A. Serra, A. Mantecon, J. Polym. Sci.: Polym. Chem. 44 (21) (2006) 6270.
[22] W. Ren, P.J. McMullan, H. Guo, S. Kumar, A.C. Griffin, Macromol. Chem. Phys. 209 (3) (2008) 272.
[23] A.R. Tajbakhsh, E.M. Terentjev, Eur. Phys. J. E 6 (2) (2001) 181.
[24] M. Tokita, H. Tagawa, H. Niwano, K. Sada, J. Watanabe, Jpn. J. Appl. Phys. 1 45 (3A) (2006) 1729.
[25] D. Rogez, H. Brandt, H. Finkelmann, P. Martinoty, Macromol. Chem. Phys. 207 (8) (2006) 735.
[26] G.H.F. Bergmann, Ph.D. Thesis, Institut fuer Makromolekulare Chemie, Freiburg, 1998.
[27] S.V. Ahir, A.R. Tajbakhsh, E.M. Terentjev, Adv. Funct. Mater. 16 (4) (2006) 556.
[28] J. Schatzle, W. Kaufhold, H. Finkelmann, Makromol. Chem. 190 (12) (1989) 3269.
[29] M. Warner, E.M. Terentjev, Liquid Crystal Elastomers, Clarendon Press, Oxford, 2003.
[30] P.G. de Gennes, in: A. Ciferri, W.R. Krigbaum, R.B. Meyer (Eds.), Polymer Liquid Crystals, Academic Press Inc., New York, 1982, p. 115.
[31] J.M. Adams, M. Warner, Eur. Phys. J. E 16 (1) (2005) 97.
[32] D.R.M. Williams, M. Warner, J. Phys. (Paris) 51 (4) (1990) 317.
[33] M.H. Li, A. Brulet, P. Davidson, P. Keller, J.P. Cotton, Phys. Rev. Lett. 70 (15) (1993) 2297.
[34] A. Greiner, H.W. Schmidt, in: D. Demus, J. Goodby, G.W. Gray, H.-W. Spiess, V. Vill (Eds.), High Molecular Weight Liquid Crystals, Wiley-VCH, Weinheim, 1998, p. 1.
[35] A. Sirigu, in: A. Ciferri (Ed.), Liquid Crystallinity in Polymers, VCH Publishers, New York, 1991, p. 261.
[36] V. Percec, M. Kawasumi, Macromolecules 24 (23) (1991) 6318.
[37] J. Kupfer, H. Finkelmann, Makromol. Chem., Rapid Commun. 12 (12) (1991) 717.
[38] C. Aguilera, J. Bartulin, B. Hisgen, H. Ringsdorf, Makromol. Chem. 184 (2) (1983) 253.
[39] P.G. de Gennes, Mol. Cryst. Liq. Cryst. 12 (3) (1971) 193.
[40] P.G. de Gennes, J. Probst, The Physics of Liquid Crystals, second ed.). Clarendon Press, Oxford, 1993.
[41] M. Warner, K.P. Gelling, T.A. Vilgis, J. Chem. Phys. 88 (6) (1988) 4008.
[42] R. Lovell, G.R. Mitchell, Acta Crystallogr., A 37 (1981) 135.
[43] G.R. Mitchell, A. Windle, in: D.C. Basset (Ed.), Developments in Crystalline Polymers, Elsevier Applied Science, New York, 1988.
[44] A. Lebar, Z. Kutnjak, S. Zumer, H. Finkelmann, A. Sanchez-Ferrer, B. Zalar, Phys. Rev. Lett. 94 (2005) 19.
[45] H. Brandt, Ph.D. Thesis, Institut fuer Makromolekulare Chemie, Freiburg, 2004.
[46] K.C. Lim, J.T. Ho, Mol. Cryst. Liq. Cryst. 47 (3–4) (1978) 173.
[47] X.J. Wang, M. Warner, J. Phys. A: Math. Gen. 19 (11) (1986) 2215.
[48] M. Warner, J.M.F. Gunn, A.B. Baumgartner, J. Phys. A: Math. Gen. 18 (15) (1985) 3007.
[49] E.R. Zubarev, R.V. Talroze, T.I. Yuranova, N.A. Plate, H. Finkelmann, Macromolecules 31 (11) (1998) 3566.
[50] H. Finkelmann, A. Greve, M. Warner, Eur. Phys. J. E 5 (3) (2001) 281.